European Review for Medical and Pharmacological Sciences 2022; 26: 8644-8659

Pentoxifylline and its association with kaempferol improve NASH-associated manifestation in mice through anti-apoptotic, anti-necroptotic, antioxidant, and anti-inflammatory mechanisms

A.O. HAMOUDA[1], A.R. ABDEL-HAMED[2], D.M. ABO-ELMATTY[2], N.F. KHEDR[3], M.H. GHATTAS[4]

[1]Department of Biochemistry, Faculty of Pharmacy, Horus University, New Damietta, Egypt
[2]Department of Biochemistry, Faculty of Pharmacy, Suez Canal University, Ismailia, Egypt
[3]Department of Biochemistry, Faculty of Pharmacy, Tanta University, Tanta, Egypt
[4]Department of Medical Biochemistry, Faculty of Medicine, Port Said University, Port Said, Egypt

Abstract. – OBJECTIVE: Non-alcoholic fatty liver disorders (NAFLD), particularly non-alcoholic steatohepatitis (NASH), have emerged as a leading cause of liver transplantation and mortality. However, the pathophysiology of NASH remains unknown. Oxidative stress, apoptosis, and necroptosis pathways are heavily linked to NASH. Therefore, the current study aimed to investigate the underlying mechanism for Pentoxifylline's (PTX) activity in NASH management, either alone or in combination with Kaempferol (KP).

MATERIALS AND METHODS: A total of 32 male C57BL/6J mice were divided into four groups: the mice in the control group were fed a standard chow diet and given a vehicle; the mice in NASH group were maintained on NASH protocol for 25 days; the mice in the PTX group were kept on NASH protocol for 25 days and given PTX (100 mg/kg), and PTX+KP mice group were given NASH protocol along with KP (50 mg/kg) and PTX (100 mg/kg) simultaneously.

RESULTS: The LDL-C, total cholesterol, triglycerides, glutathione peroxidase (GPx), superoxide dismutase (SOD), malondialdehyde (MDA), glucose, insulin, and HOMA-IR levels were considerably decreased in the PTX and PTX+KP treated groups. AMP-activated protein kinase (AMPK) Gene expression of the liver was significantly increased in the other treated groups, but peroxisome proliferator-activated receptor (PPAR), phosphorylated mixed lineage kinase-like protein (pMLKL), and sterol regulatory element binding protein 1 (SREBP1) were reduced significantly. Caspase-8 and receptor-interacting serine/threonine protein kinase (RIPK3) protein expression were significantly decreased in the PTX and PTX+KP groups compared to NASH group and nuclear factor kappa B (NF-κB), interleukin-6 (IL-6), and tumor necrosis factor alpha (TNF-α) immunohistochemistry expression.

CONCLUSIONS: Our current study suggests that PTX and its combination with KP have a significant ameliorative effect against NASH *via* novel mechanisms involving the regulation of apoptosis and necroptosis, as well as decreased oxidative stress, lipogenesis, proinflammatory cytokines, and modulation of histopathological manifestation.

Key Words:
Apoptosis, Kaempferol, Necroptosis, Inflammation, NASH, Pentoxifylline, Oxidative stress.

Introduction

Non-alcoholic fatty liver disorder (NAFLD) is a complex disorder, with clinical signs becoming serious only when the condition progresses to non-alcoholic steatohepatitis (NASH), when liver damage, inflammation, and fibrosis are overlaid on the initial steatosis[1]. NASH develops and progresses due to inflammatory processes, supporting the condition's progression toward more severe disorders, including cirrhosis and hepatocellular cancer (HCC)[2]. Progressive steatohepatitis is brought on by the widespread apoptosis that free fatty acids inflict on hepatocytes[3].

Human NASH also exhibits necrosis and necro-inflammation, indicating that different cell death mechanisms may contribute to the disease's etiology[4]. Mixed lineage kinase domain-like

Corresponding Author: Amir O. Hamouda, MD; e-mail: Ahamouda@horus.edu.eg

(MLKL) and receptor-interacting serine/threonine protein kinase (RIPK3) expression were also important in human non-alcoholic steatohepatitis (NASH) situations. Necroptosis is a key form of programmed cell death that is required to regulate inflammation in many tissues such as the skin and gastrointestinal tract. Furthermore, necroptosis is triggered in alcoholic liver injury. However, the significance of RIP3 in NASH is still unknown[5].

In NASH clinical trials, several new apoptosis inhibitors have been attempted, but no meaningful protective effect has yet been found. In a mice alcohol-induced liver injury model, blocking caspase-8 reduces hepatic cell death, implying a transition from apoptosis into necroptosis[6].

AMP-activated protein kinase (AMPK) is an important energy sensor that controls metabolic balance. Recent literature suggests that AMPK activity is suppressed during metabolic diseases such as obesity, diabetes, and NAFLD[7]. AMPK suppression links lipid imbalance to inflammation, liver damage, and fibrosis in NASH[8]. However, pharmacological AMPK activation improves NASH in both murine and simian models. Moreover, in hepatocytes exposed to high glucose, AMPK increases Ser372 phosphorylation, inhibits sterol regulatory element-binding proteins (SREBP-1c) breakage and nuclear translocation, and represses SREBP-1c target gene expression, decreasing the lipogenesis and lipid buildup[9].

Recently, several investigations[10,11] have found that oxidative stress is a significant factor in the development from steatosis to steatohepatitis. Mitochondria play a crucial role in FFA oxidation[10]. However, mitochondria produce reactive oxygen species (ROS), often in the form of hydrogen peroxide (H_2O_2), during the FFA oxidation process. ROS also stimulates the generation of cytokines such as tumor necrosis factor gamma (TNF-γ), transforming growth factor beta (TGF-ß), and interleukin-8 (IL-8), which all induce hepatocyte death and hepatitis[12].

Pentoxifylline (PTX) is a methylxanthine derivative with strong hemorrhagic characteristics frequently used to treat intermittent claudication. Recent research in both humans and animals suggest that PTX may cause several cellular physiological changes, including c-AMP through activation of phosphodiesterase-4 (PDE-4) and TNF-α gene transcription, inhibition of nuclear factor kappa B (NF-κB), modulation of cytokines and chemokines production; all of which are relevant to the mechanisms of NASH[13]. Therefore, the effectiveness of pentoxifylline therapy in NASH has become a research hotspot.

Kaempferol is a naturally occurring flavonoid in broccoli, tea, and other plants[10]. Notably, this molecule has several biological and pharmacological actions, including antioxidant and anti-inflammatory activity and the ability to limit tumor growth[14]. Kaempferol can protect normal liver cells against cytotoxicity, ROS production, and DNA damage caused by H_2O_2[15].

Overall, the current study aimed to investigate the underlying mechanism for Pentoxifylline's (PTX) activity in NASH management, either alone or in combination with Kaempferol (KP).

Materials and Methods

Chemicals and Drugs

Chemicals and pharmaceuticals were of excellent analytical grade and purchased from reputable commercial sources. Kaempferol (KP) was acquired from AdooQ Bioscience, (Irvine, CA, USA). The liver X receptor (LXR) agonist (T0901317) was purchased from AdooQ Bioscience, (Irvine, CA, USA). PTX was a gift from Sigma Pharmaceutical Company, (Naser City, Cairo, Egypt). Carbon tetrachloride (CCl_4) was obtained from Biodiagnostic Co., (Dokki, Giza, Egypt). Dimethyl sulfoxide (DMSO) purchased from Sigma Aldrich, (St.Louis, MO, USA) was used as a vehicle for the preparation of pentoxifylline, LXR agonist (T0901317) and KP.

Animals

Thirty-two C57BL/6J mice aged eight-week-old and weighing (25-34 gm) were provided from Medical Experimental Research Center (MERC) (First District, Mansoura, Egypt). Mice were acclimatized for one week and provided with normal food chow and tap water *ad libitum* at a 12-hour light/dark cycle and 25C°.

NASH Induction

In brief, mice were fed a high-fat diet (20% protein, 60% fat, and 20% carbohydrate equivalent to 3.6 Kcal/g) which was purchased from Research Diets Inc, (New Brunswick, New Gersy, USA) (Table I). Then, mice were taken four intraperitoneal (Ip) injections of 0.1 mL/kg/bw of carbon tetrachloride CCl_4 to develop NASH on 14^{th}, 17^{th}, 21^{st}, and 24^{th} days from the beginning

Table I. The ingredients of a normal high-fat diet (HFD) and chow diet.

Class descriptiont	Normal chow diet	High-fat diet
Protein	29%	21%
Carbohydrates	56%	20%
Fats	4.5%	61%
Calories	864 Kcal	4,041 Kcal

of experiment. Whereas liver X receptor (LXR) agonist (T0901317) was administered five times (Ip) on 20th -24th days at a dose of 2.5 mL/kg[16].

Animal Groups

Mice were randomly assigned into four groups according to treatments (n=8).

Control: mice received DMSO as a vehicle with a normal chow diet.
NASH: mice received NASH protocol daily for four weeks.
PTX: mice received PTX (100 mg/kg) daily via oral gavage for four weeks parallel with the NASH protocol[17].
PTX+KP: mice received an oral daily dose of PTX (100 mg/kg) plus orally dose of KP (40 mg/kg) for four weeks parallel with the NASH protocol.

All treatments were started on the 24th day after the beginning of NASH protocol and lasted for a month. Weights of the animals were recorded every week.

Collection of Samples

At the end of the experiment, animals were starved overnight. Blood was taken from the retro-orbital plexus. For biochemical analysis, serum was isolated and kept at 20°C. Animals were slaughtered, and their livers were harvested, rinsed with normal saline, and sliced into little pieces. One piece was fixed in 10% formalin for histological examination, while the remaining sections were stored at -80°C for Western blotting and reverse transcription polymerase chain reaction (RT-PCR) analysis.

Determination of Liver Function Indices and Lipid Profile

Serum total cholesterol (TC), triglycerides (TG), high-density lipoprotein-cholesterol (HDL-C), low dentistry lipoprotein-cholesterol (LDL-C), alanine aminotransferase (ALT), and aspartate transaminase (AST) were determined using a FUJI DRI-CHEM 7000 automated chemistry analyzer (Fujifilm Corp, Minato, Tokyo, Japan).

Determination of Blood Glucose Homeostasis

For determination of glucose homeostasis, fasting blood glucose, fasting insulin, and HOMA-IR were measured. The enzymatic colorimetric technique reported by Trinder was used to test fasting plasma glucose levels using kits from Biovision Company, (Naser City, Cairo, Egypt)[18]. Insulin level using a rat insulin enzyme-linked immunosorbent assay (ELISA) kit provided by Adooq Biosciences Inc Co., (Irvine, CA, USA) according to the manufacturer's procedure. HOMA-IR was calculated using the reported formula according to Matthews et al[19].

Gene Expression of PPAR, AMPK, SREBP1, and pMLKL by Quantitative Real-Time Reverse Transcriptase Polymerase Chain Reaction (qRT-PCR)

Total RNA was isolated from homogenized liver tissues according to the instructions of the manufacturer using VWR Life Science RiboZol™ RNA Extraction Reagent from Thermo Fisher Scientific. The RevertAidTM First Strand cDNA Synthesis kit (Thermo Fisher Scientific, Wilmington, MA, USA) was used to create the cDNAs. The Real-Time PCR Detection System was used to perform real-time PCR using the Thermo Fisher Scientific Maxima SYBR Green qPCR Master Mix and the appropriate primers (Wilmington, MA, USA). The primer sets utilized as follows: PPAR forward primer, 5′-TGTGGGGATAAAGCATCAGGC-3' and reverse primer, 5′-CCGGCAGTTAAGATCACACCTAT-3', AMPK forward primer, 5′-CTCAGTTCCTGGAGAAAGATGG-3' and reverse primer, 5′-CTGCCGGTTGAGTATCTTCAC-3'. SREBP1 forward primer, 5′-GGAGCCATGGATTGCACATT-3' and reverse primer, 5′-GGCCCGGGAAGTCACTGT-3'. pMLKL forward primer, 5′-CTGAGGGAACTGCTGGATAGAG-3' and reverse primer, CGAGGAAACTGGAGCTGCTGAT. β-actin forward primer, 5′-ACTATTGGCAACGAGCGGTT-3' and reverse primer, 5′-CAGGATTCCATACCCAAGAAGGA-3'. The SYBR green values were quantified relative to β-actin as a reference gene. The samples' threshold cycle (Ct) values were computed, and tran-

script levels were determined using the $2^{-\Delta Ct}$ method[20]. The Primer 3 tool was used to create these primers based on previously known mouse sequences (available at: http://www-genome.wi.mit.edu/cgi-bin/primer/primer3). We utilize BLAST (available at: www.ncbi.nlm.nih.gov/blast/Blast.cgi) to compare the primer and template sequences to other known sequences to check that they were unique.

Preparation of Liver Homogenate

The liver tissues were quickly removed and washed in ice-cold sterile physiological saline water (0.9%). After preparing a 10% homogenate in 0.1M sodium phosphate buffer (pH 7.4) was centrifuged at 3,000 rpm for 15 min at 4 C˚ using a Beckman colter centrifuge from (Beckman colter life sciences, Indianapolis, USA) (rotor radius: 20.4 cm). The supernatant was utilized for further investigation[21].

Superoxide Dismutase Activity (SOD)

SOD activity was measured using a commercial kit (Biodiagnostics Co., Dokki, Giza, Egypt)[22]. Liver homogenates were mixed with Tris-HCl (pH 8.2) and pyrogallol (15 mM), and the absorbance was measured at 420 nm for 3 min against a blank. SOD activity was measured in mg/g tissue. One unit of SOD is defined as the amount of enzyme that prevents 50% of pyrogallol oxidation.

Determination of Malondialdehyde (MDA)

Lipid peroxidation marker MDA from Biodiagnostics Co., (Dokki, Giza, Egypt) was measured as a thiobarbituric acid reactive substances and quantified as MDA equivalents using 1,1,3,3-tetra methoxy propane as a reference. The data were given in nmol/g tissue[23].

Determination of Glutathione Peroxidase (GPx)

The enzyme reaction of GPx included NADPH, reduced glutathione, sodium azide, and glutathione reductase, then the reaction was started using H_2O_2, and the change in absorbance at 340 nm was measured using a DLAB SP-UV1100 Spectrophotometer (MediLab Tech Co., CA, USA) spectrophotometer. The activity was expressed as units per gram of tissue. A commercial kit was used to measure GPx activity indirectly from Biodiagnostic Co., (Dokki, Giza, Egypt)[24].

Histopathological Examination

The liver tissues were fixed and embedded in paraffin using standard procedures. Three µm thick paraffin slices of the liver were cut using a microtome (Leica RM2135, Wetzlar, Germany). Sections were stained with hematoxylin and eosin (H&E) to evaluate inflammation and hepatocellular ballooning. A qualified pathologist, who is blinded to the treatment, assessed the liver sections. The stained slides were inspected using a BZ-9000 BioRevo digital microscope (Keyence Corp., Osaka, Japan), and the images were processed with ImageJ. The NAFLD activity score was calculated by analyzing the degree of liver steatosis, inflammation, and ballooning of the NASH score[25].

IL-6, TNF-α, and NF-κB Immunohistochemistry in Liver Tissue

Liver paraffin slides were deparaffinized and rehydrated on positively charged glass slides in absolute methanol. Endogenous peroxidase is inactivated, and sections were incubated in 0.3% H_2O_2 for 30 min. Sections were incubated in 5% skimmed milk for 30 min at room temperature. Using a microwave, the antigen was extracted for 15 min in a 10 mM citrate buffer. Diluted TNF-α (1:100), IL-6 (1:50), and NF-κB primary antibodies (Abcam, Cambridge, Massachusetts, USA) were then applied to the sections overnight at 4°C (1:150). After washing with PBS, the slides were incubated with the secondary antibodies (Abcam, Cambridge, Massachusetts, USA) at room temperature for 30 min. After applying 3-diaminobenzidine for 2-4 min and rinsing in distilled water, the brown color form was counterstained with Mayer's hematoxylin for 1 min at room temperature. The positively stained area was brown, unlike the negatively stained zone. Finally, the intensity of the colors was assessed using the image analyzer "Image J Program" (Abcam, Cambridge, MA, USA).

Western Blotting of Caspase 8 and RIPK3

Liver tissues were lysed and then put on ice for 30 min at -80°C. The lysates were centrifuged at 4°C for 30 min at 15,000 rpm/min. The conventional western technique was followed. The polyvinylidene fluoride membranes were treated with primary antibodies such as anti-caspase eight and anti-RIPK3 (Santa Cruz Biotechnology inc., Dallas, Texas, USA). The next day, the β-actin mono-

clonal antibody (Santa Cruz Biotechnology inc., Dallas, Texas, USA) was added and incubated for 1 hour. The appropriate secondary antibody was applied to each membrane (horseradish peroxidase-conjugated goat anti-rabbit IgG). Image J software was used to assess the density of the protein of the interest band, which was then normalized to the β-actin protein band[26].

Statistical Analysis

One-way ANOVA was used to examine the data, followed by the Dunnett Multiple Comparison Test. Means ± SD was used to depict the values. GraphPad Prism software version 5 was used for statistical analysis (San Diego, CA, USA). The differences were judged significant when the estimated *p*-value was lower than 0.05.

Results

Effect of Treatment on Body Weight, Liver to the Weight of the Body, and Liver Weight

The mean body weight of all groups during the 8 weeks of the experiment is shown in Table II. Compared to the control group, the NASH group's final body weight increased by 20% ($p>0.001$). Compared to NASH group, the PTX and PTX+KP groups reduced the ultimate weight of the body by 10% and 13%, respectively ($p>0.001$).

The NASH group has 222% ($p>0.001$) increase in liver weight compared to control group. Compared to the NASH group, the PTX and PTX+KP groups showed a significant reduction in the weight of the liver by 41.3% and 48.2% ($p>0.001$), respectively, compared to the untreated NASH group.

Surprisingly, when compared to the NASH group, the PTX and PTX+KP treated groups had a substantial drop in the Liver/BW ratio of 33.16% and 39.35% ($p>0.001$), respectively. The percent change in the weight of the PTX and PTX+KP treated groups was considerably lower than in the NASH group, by 63.7% and 82.1% ($p>0.001$), respectively.

Effect of Treatment on Glucose Homeostasis

Plasma glucose and insulin levels are illustrated in Figures 1A and B. The untreated NASH group had 90.5% and 74% ($p>0.001$) higher glucose and insulin levels than the control group. In comparison to the NASH group, the PTX and PTX+KP groups showed a substantial reduction in fasting plasma glucose of 6.5% and 17% ($p>0.001$), respectively.

PTX and PTX+KP successfully decreased the elevated insulin levels caused by the NASH diet to 10.1% and 15.2% ($p>0.001$), lower than the group NASH, respectively. In comparison to the group of NASH, the HOMA-IR values in the PTX and PTX+KP groups were lower by 20.6% and 29.9%, respectively ($p>0.001$). Figure 1C depicts the change in the HOMA-IR score across all groups investigated ($p>0.001$).

Effect of Treatment on Lipid Profile

Compared to the normal control group, the untreated NASH group had remarkable increases in plasma TC, TG, and LDL-C of 191.3%, 413.1%, and 332.5%, respectively. Furthermore, the NASH group's HDL-C levels were 41% lower than the control group ($p>0.001$).

When compared to the NASH group, plasma TGs were lowered by 68.5% and 70% ($p>0.001$)

Table II. Effect of treatment on body weight, liver weight, and percent of weight change.

Measure	Control	NASH	PTX	PTX+KP	Test of significance
Liver weight	0.9 ± 0.01	3 ± 0.01[a]	1.7 ± 0.1[abde]	1.5 ± 0.1[abc]	$p < 0.001$
Final body weight	30 ± 1.1	36 ± 1[a]	32.1 ± 1[ab]	31.3 ± 0.5[abc]	$p < 0.001$
Liver/BW	0.028 ± 0.008	0.081 ± 0.002[a]	0.054 ± 0.002[ab]	0.049 ± 0.002[abc]	$p < 0.001$
Percent of weight change	2.61, -9.7, 7.1	19.5, 13.3, 29.8[a]	6.7, 0, 13.3[ab]	3.3, -1.5, 6.7[bc]	$p < 0.001$

Except for % of weight change, which is shown as median (min, max), other measurements are expressed as mean± (SD) (n=8). [a]= significance *vs*. Control group, [b]= significance compared NASH group, [c]= significance *vs*. Pentoxifylline group. Control group: normal chow diet-fed mice for four weeks; NASH group: mice received high fat diet-fed, CCL4 (0.1 mg/kg) four times (day 20-24) and T0903156 (2.5 mg/kg) five times only for four weeks, PTX: Mice received Pentoxifylline (100 mg/kg); PTX+KP group: (NASH+PTX+KP). The treatments were given orally every day for four weeks, in conjunction with the NASH diet.

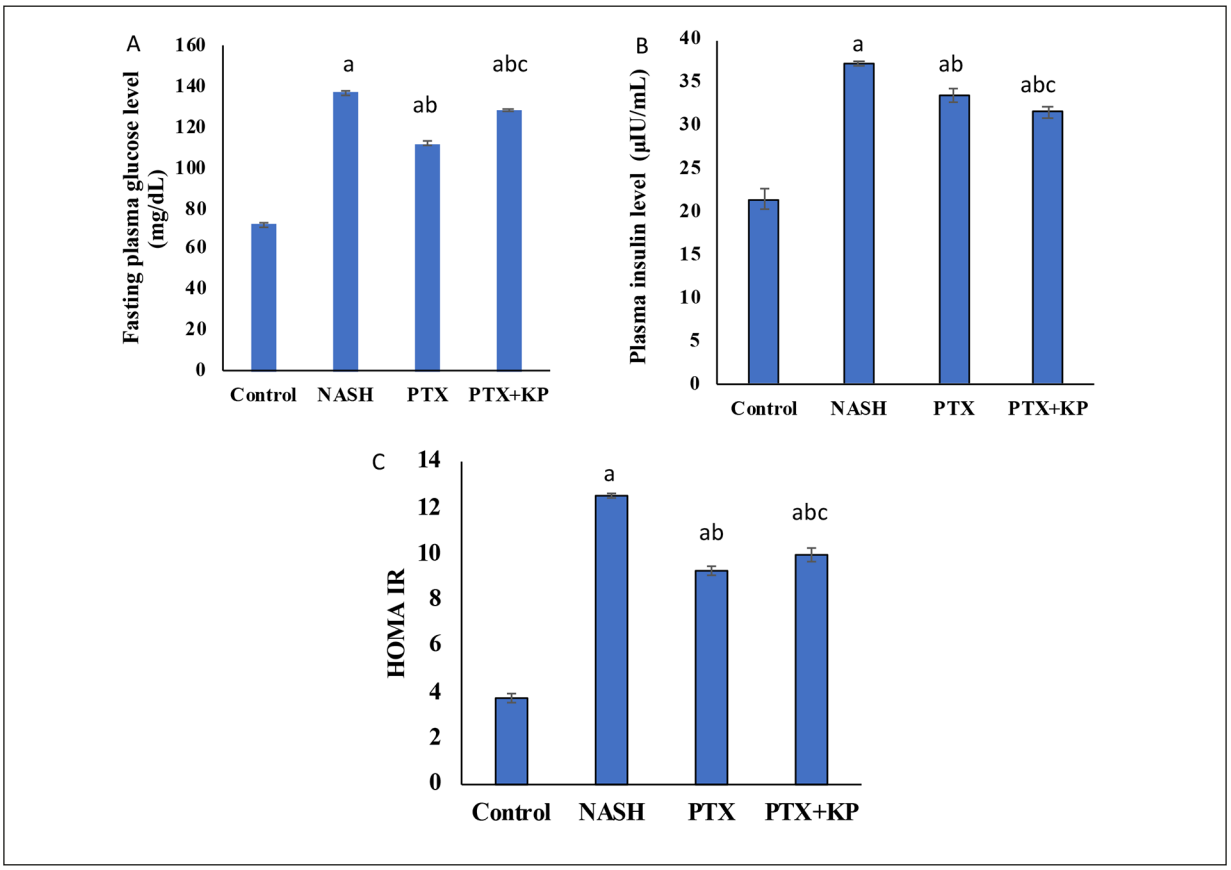

Figure 1. A, Fasting plasma glucose level in mice groups. **B,** Plasma insulin level in mice groups. **C,** HOMA-IR in mice groups. Data are represented as a mean ± SD (n=8/group), and significance was set at $p<0.05$. a: significant *vs.* control group, b: significant *vs.* NASH group, c: significant *vs.* PTX group. NASH: nonalcoholic steatohepatitis, PTX: Pentoxifylline, KP: Kaempferol.

in the PTX and PTX+KP groups, respectively. PTX and PTX+KP treatment groups showed 32.2% and 36.3% lower levels of TC, respectively, than the NASH control group ($p>0.001$).

Similarly, the PTX and PTX+KP groups significantly lowered LDL-C levels by 12.9% and 21.5%, respectively, compared to the NASH group ($p>0.001$). PTX and PTX+KP therapy enhanced plasma HDL-C levels by 17.3% and 27.2%, respectively, when relevant to the NASH group ($p>0.001$) (Figure 2A).

Effect of Treatment on Liver Enzymes

The PTX and PTX+KP groups lowered plasma ALT by 89.3% and 89.9%, respectively, compared to the NASH group. Furthermore, AST levels in the PTX and PTX+KP treated groups were lowered by 84.9% and 86.7%, respectively, when compared to the NASH group ($p>0.001$) (Figure 2B).

Effect of Treatment on AMPK, PPAR-γ, SREBP-1, pMLKL

As shown in Figure 3 PTX and PTX+KP decreased PPAR-γ expression in the liver by 45.9% and 74.6% ($p>0.001$), respectively compared to NASH group. In comparison to NASH group, SREBP1 gene expression in PTX and PTX+KP groups was suppressed by 33.2% and 69.4%, respectively ($p>0.001$). Similarly, PTX and PTX+KP treatment reduced pMLKL expression by 24.1% and 29.4%, respectively ($p>0.001$) in comparison to NASH group. PTX and PTX+KP up-regulated AMPK gene expression by 221% and 105.2%, respectively, as compared to untreated NASH group ($p>0.001$).

Effect of Treatment on the Expression of RIPK3 and Caspase 8 Proteins in Liver Tissue

When compared to the NASH group, PTX and PTX+KP groups had reduced RIPK3

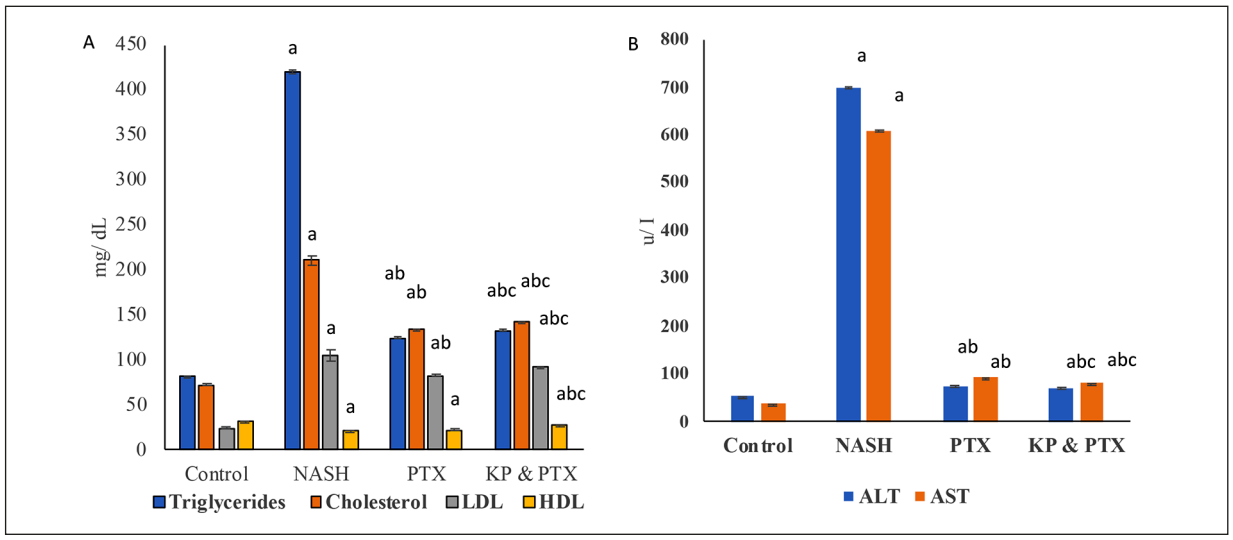

Figure 2. A, Plasma lipid profile in mice groups; **B,** serum liver enzymes ALT and AST levels in mice groups. Data are represented as a mean ± SD (n=8/group), significance was set at $p<0.05$. a: significant *vs.* control group, b: significant *vs.* NASH group, c: significant *vs.* PTX group. NASH: nonalcoholic steatohepatitis, PTX: Pentoxifylline, KP: Kaempferol.

expression by 25.4% and 47%, respectively ($p>0.001$) (Figure 4A and 4B). Furthermore, PTX and PTX+KP treatment decreased caspase-8 protein expression by 42.3% and 72%, respectively, compared to the NASH group ($p>0.001$). Combined KP+PTX therapy normalizes RIPK3 and caspase 8 expressions in treated NASH group.

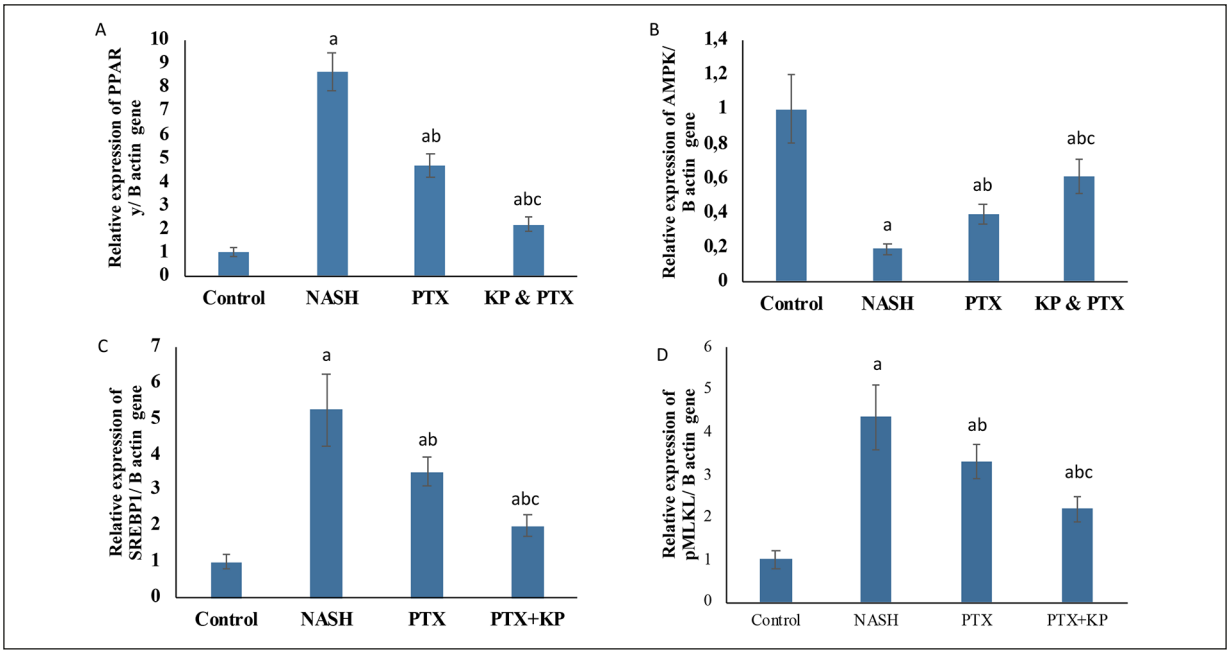

Figure 3. A, PPAR-γ subunit gene expression (relative copy number "RCN") in liver tissue of mice groups. **B**, AMPK gene expression (RCN) in liver tissue of mice groups. **C**, SREBP1 gene expression (RCN) in liver tissue of mice groups. **D**, pMLKL gene expression (RCN) in liver tissue of mice groups. Data are represented as a mean ± SD (n=8/group), significance was set at $p<0.001$. a: significant *vs.* control group, b: significant *vs.* NASH group, c: significant *vs.* PTX group. NASH: nonalcoholic steatohepatitis, PTX: Pentoxifylline, KP: Kaempferol.

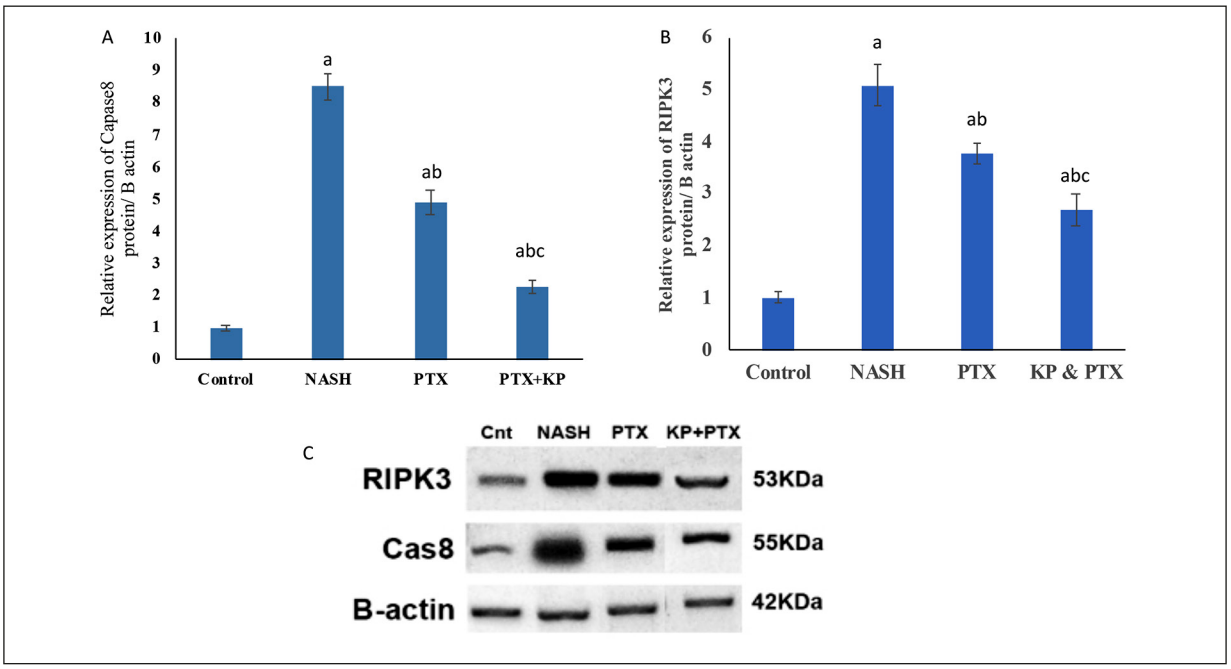

Figure 4. A, Caspase 8 protein expression in liver tissue of mice groups. **B**, RIBK3 protein expression in liver tissue of mice groups after treatment. **C**, Western blot analysis showing protein expression of RIPK, caspase 8 and β-actin in different experimental groups. Data are represented as a mean ± SD (n=8/group), significance was set at $p<0.05$. a: significant *vs.* control group, b: significant *vs.* NASH group, c: significant *vs.* PTX group. NASH: nonalcoholic steatohepatitis, PTX: Pentoxifylline, KP: Kaempferol.

Effect of Treatment on SOD, GPx and MDA in Liver Tissue

SOD activity was increased by 74.2% and 138.6% ($p>0.05$) in NASH treated groups with PTX and PTX+KP, respectively as compared to untreated NASH group (Figure 5A). PTX and PTX+KP treatment resulted in a substantial reduction in GPx activity by 24.5% and 40% ($p>0.05$), respectively compared to NASH group (Figure 5B). Treatment with PTX alone or in combination with KP, on the other hand, resulted in substantial decreases in MDA levels by 28.5% and 43.6% ($p>0.05$), respectively, compared to NASH group (Figure 5C).

Effect of Treatment on Liver Histopathology

Herein, the novel NASH model induced in mice showed bridging fibrosis, liver steatosis, macrovesicular, and hepatocytes ballooning with congestion and inflammation of the lobules (Figure 6). Furthermore, as seen in NASH group, liver steatosis had a higher lesion score (Figure 6 A-a, B-b). However, PTX and PTX+KP treated NASH groups showed reduction in liver lesion scores by 81% ($p>0.001$) and by 86% ($p>0.001$), respectively compared with untreated NASH group (Figure 6 C-D).

Effect of Treatment on Immunohistochemistry of IL-6, TNF-α, and NF-κB in Liver Tissue

When compared to NASH group, mice treated with PTX or the co-treatment with PTX and KP showed a substantial decrease in TNF-α expression by 48.3% and 78% ($p>0.001$), respectively (Figure 7). Similarly, when compared to untreated NASH group, the expression of NF-κB was reduced by 46.1% and 69.2% ($p>0.05$) in PTX and PTX+KP treated groups, respectively (Figure 8). Furthermore, treated mice groups with PTX and PTX+KP showed a substantial reduction in IL-6 expression of 49.9% and 78.5% ($p>0.001$), respectively in comparison to the NASH group (Figure 9).

Discussion

Researchers are continually looking for helpful treatments, despite the unknown underlying molecular pathway that causes NASH. Some

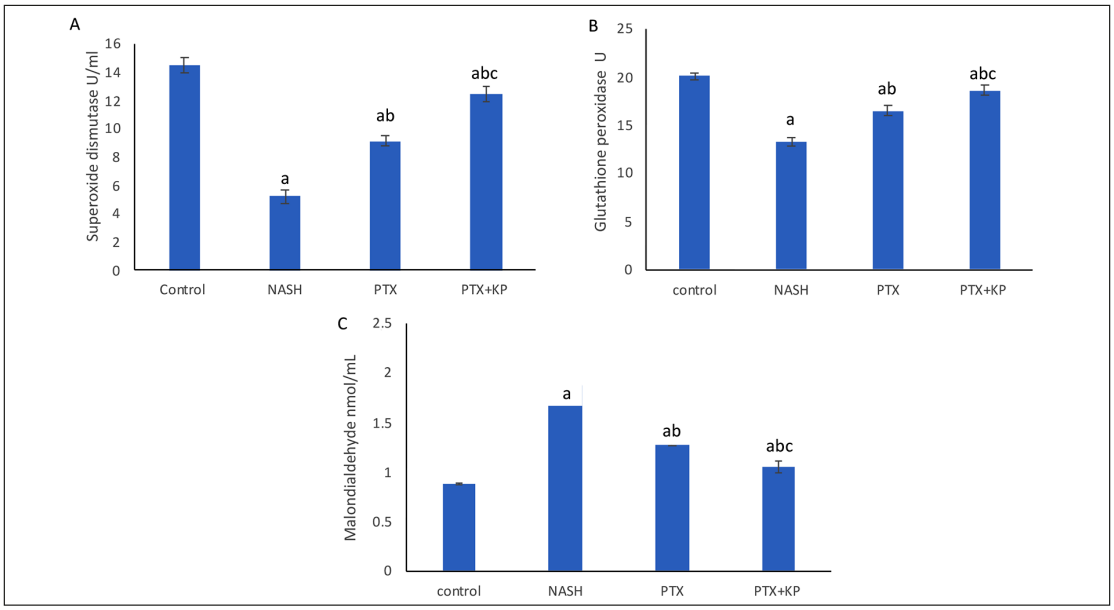

Figure 5. **A**, Superoxide dismutase levels in mice groups; **B**, glutathione peroxidase levels in mice groups. **C**, Malonaldehyde levels in mice groups. Data are presented as a mean ± SD (n=8/group), significance was set at $p<0.05$. a: significant *vs.* control group, b: significant *vs.* NASH group, c: significant *vs.* PTX group. NASH: nonalcoholic steatohepatitis, PT×Pentoxifylline, KP: Kaempferol.

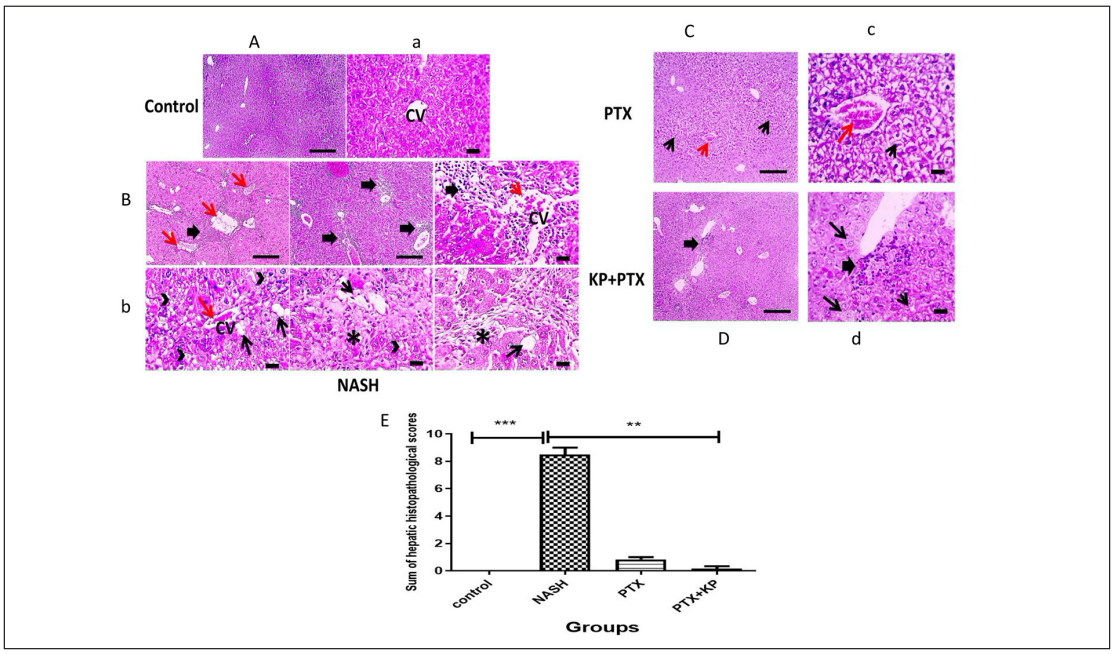

Figure 6. Microscopic pictures of H&E-stained liver sections. **A-a** show normal hepatocytes arranged in radiating plates around a central vein (CV) with normal sinusoids in control group. **B-b**, Liver sections from NASH group show marked perivascular inflammation (*thick arrows*), congested central vein (*red arrow*), micro- (*arrowheads*) to few macro-vesicular (*thin black arrow*) steatosis in hepatocytes and fibrosis (*black asterisk*). **C-c**, Liver sections from the treated groups show mildly congested blood vessels (*red arrow*), very mild portal fibrosis (*thick black arrow*), prominent hydropic degeneration in hepatocytes (*thin black arrow*) in the PTX group. **D-d**, Liver sections from PTX+KP show few perivascular leukocytic cells infiltration (*thick arrows*), mild hydropic degeneration (*long black arrow*) and scattered macrovesicular steatosis in hepatocytes (*short black arrow*) in KP+PTX group. Low magnification ×100 bar 100, high magnification ×400 bar 50. **E**, Statistical analysis of histopathological lesional scores in H&E-stained hepatic sections showing significantly higher scores in NASH group when compared with control group. Significant reduction of hepatic lesional scores is seen in the treated group with PTX+KP when compared with NASH group. **Mean significant when $p<0.01$ and ***mean significant when $p<0.001$

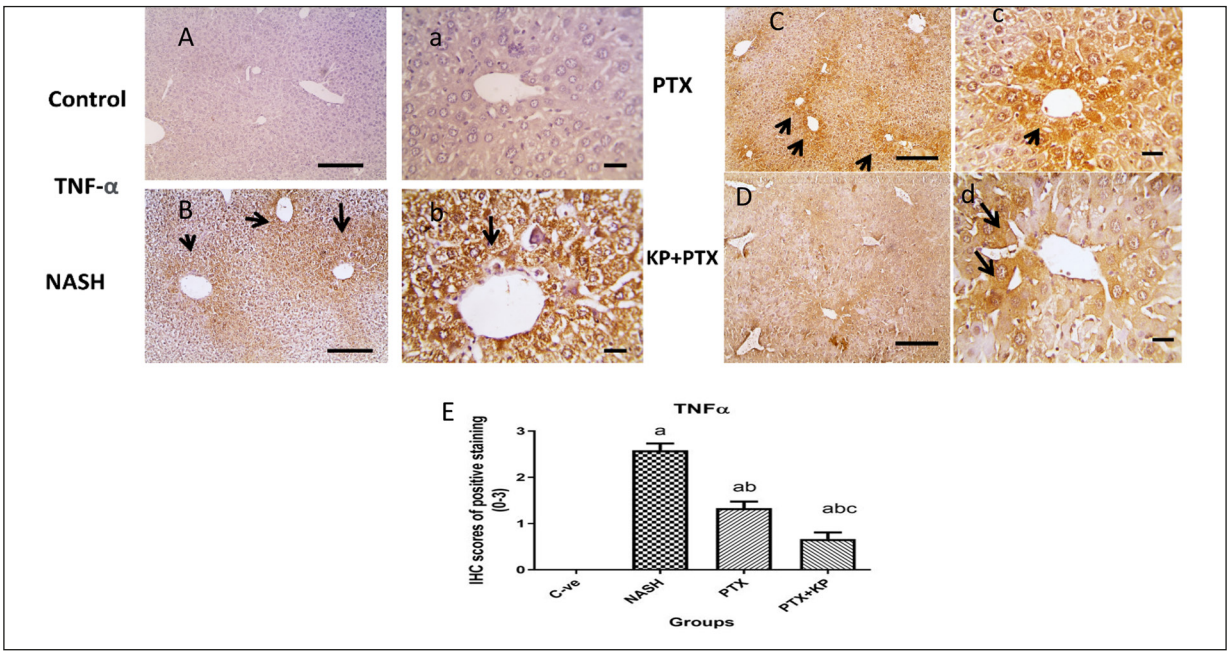

Figure 7. Microscopic pictures of immunostained liver sections against TNF-α (Low magnification ×100 bar 100, high magnification ×400 bar 50) showing: (**A**, **a**) control group showed negative staining. **B**, **b**, NASH group showed marked positive brown expression against TNF-α in hepatocytes (*black arrows*) (**C**, **c**) PTX group showed decreased positive brown expression in hepatocytes (*black arrows*) in treated groups with a single drug, (**D**, **d**) PTX+KP group showed much more decreased of positive brown expression in hepatocytes (*black arrows*) in treated groups with drug combinations. IHC counterstained with Mayer's hematoxylin. **E**, Statistical analysis of positive IHC expression scores of TNF-α with the Kruskal-Wallis method (found to be non-parametric data) followed by Dunn's test showed a significant increase in NASH compared to the control group. Significant reductions of positive IHC expression scores of IL-6 in treated groups with drug combinations to be the lowest in treated group with PTX+KP. Small alphabetical letters mean significant when $p<0.05$. Data are presented as mean ± SD, $p<0.001$, n = 8. a: significant *vs.* control group, b: significant *vs.* NASH group, c: significant *vs.* PTX group.

studies[27] have found that natural flavonoids can treat and prevent liver diseases. Our work aimed to look at the effects of PTX on a liver-induced NASH model alone and in combination with KP, as well as the different mechanisms, which included oxidative stress necroptosis and apoptosis pathways[28].

Several diets and drug-induced animal models have been used because of their morphologic and histopathologic similarities to human NASH. Fat buildup in hepatocytes is important in the development of NASH. Herein, the triple combination of dietary and chemical inducers produced human-like NASH model in mice in four weeks. The liver X receptor agonist (T0901317) stimulates liver *de novo* lipogenesis when administered orally according to Owada et al[15]. In addition, the high fructose (HF) diet increases fatty acid intake and increases the development hepatic steatosis necroptosis, apoptosis, and cirrhosis. Therefore, we aimed to analyze the protective effects of PTX alone and in combination with KP on the liver in NASH-induced mice model and the underlying mechanisms.

Kaempferol has been reported[29] to decrease fat in the body by decreasing lipogenesis, boosting lipolysis, and limiting the growth of preadipocytes. In comparison to NASH group, PTX and KP+PTX therapy significantly decreased final body weight and liver weights, a finding that was more in the PTX+KP group. These findings agreed with those reported in previous studies[30].

Herein, the histological findings demonstrated that PTX may benefit hepatic steatosis. Moreover, when PTX combined with KP we discovered that co-therapy had more influence on normalizing the body and liver weights. This is due to the combined activities of the two drugs, which work through different mechanisms.

PTX is a phosphodiesterase inhibitor with a wide variety of reported immunomodulatory, antioxidant, and anti-inflammation effects. It is a

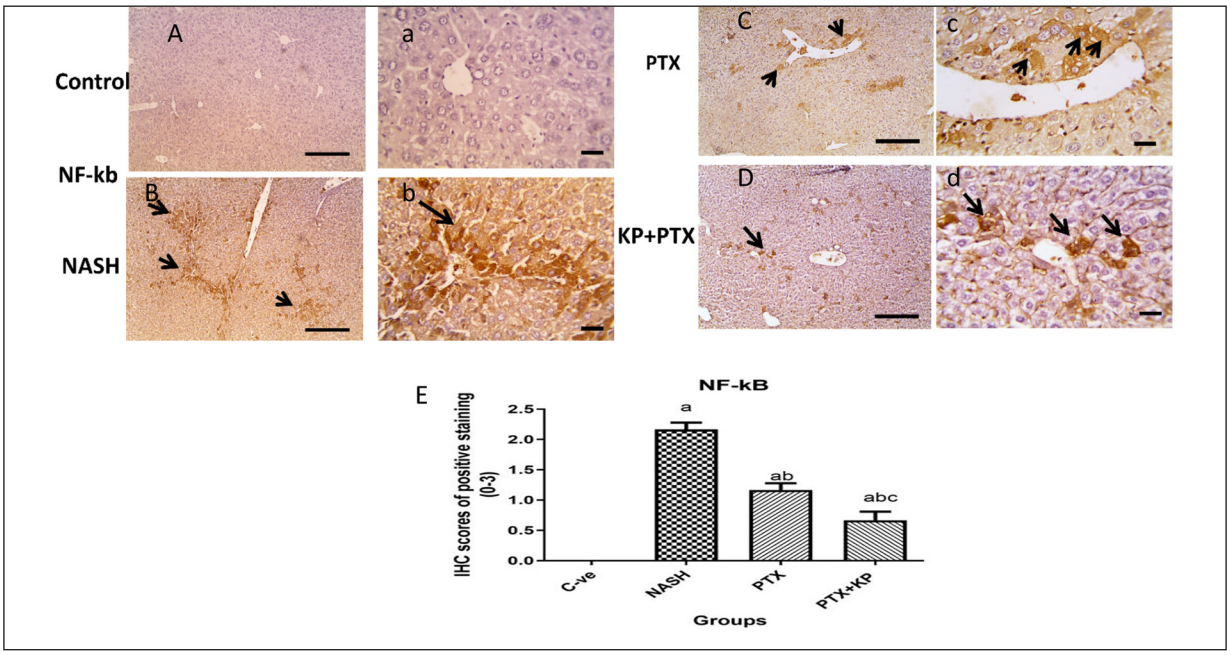

Figure 8. Microscopic pictures of immunostained liver sections against NF-κB (Low magnification ×100 bar 100, high magnification ×400 bar 50) showing: control group showed negative staining (**A-a**); NASH group showed marked positive brown expression against NF-κB in hepatocytes (*black arrows*) (**B-b**); PTX group showed decreased positive brown expression in hepatocytes (*black arrows*) in treated groups with a single drug (**C-c**); PTX+KP group showed much more decreased of positive brown expression in hepatocytes (*black arrows*) in treated groups with drug combinations (**D**, **d**). IHC counterstained with Mayer's hematoxylin. **E**, Statistical analysis of positive IHC expression scores of NF-κB with the Kruskal-Wallis'method (found to be non-parametric data) followed by Dunn's test showed a significant increase in NASH compared to the control group. Significant reductions of positive IHC expression scores of IL-6 in treated groups with drug combinations to be the lowest in treated group with PTX+KP. Small alphabetical letters mean significant when $p<0.05$. Data are presented as mean ± SD, $p<0.001$, n=8. a: significant *vs.* control group, b: significant *vs.* NASH group, c: significant *vs.* PTX group.

common therapy for peripheral vascular disease. In rat liver damage, the protective effect of PTX was recently proven to preserve the liver function including ALT and AST[31]. These enzymes are secreted into the bloodstream by injured hepatocytes and have been used as critical biomarkers to assess the degree of hepatic injury[32]. These data supported our investigation that oral treatment of PTX reduced serum elevations of ALT and AST caused by NASH. Meanwhile, the histopathological findings in the present study showed decreased hepatocellular inflammation and steatosis after treatment with PTX and PTX+KP[33].

In the current investigation, insulin resistance was much greater in the NASH group, as shown by higher insulin resistance (HOMA-IR) values. The current study discovered that giving PTX to mice fed a NASH diet resulted in reduced fasting glucose and insulin levels, which were highly significant. PTX alone and PTX+KP may boost insulin signal transduction in adipocytes by stimulating the expression of genes related to increased glucose level and glucose transporter type 4 translocation. Also, PTX improves glucose management and HOMA-IR. An earlier study[34] on the effects of PTX on glucose metabolism found that it decreases blood glucose *via* increasing intracellular cAMP levels and insulin production.

Kaempferol improves diabetes by inhibiting the pathway of NF-κB activation. This may help to lower the number of lesions in the liver, which may help to improve insulin signaling problems in diabetes patients according to Luo et al[35]. Furthermore, previous research[36] discovered that KP reduced inflammatory cytokine expression and glucose-induced ROS generation. Moreover, adding KP to PTX was thought to increase insulin secretion and enhance peripheral glucose consumption[37].

Regarding the lipid profile examined in this study, PTX-treated mice had lower TGs, LDL-C,

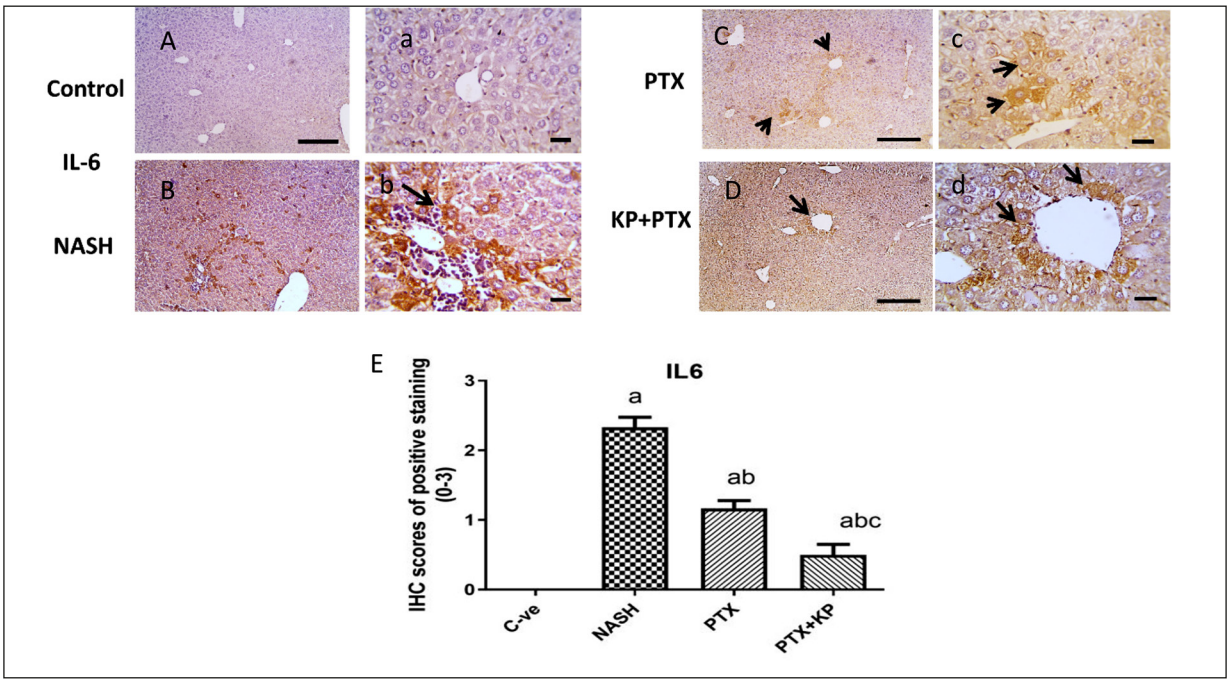

Figure 9. Microscopic pictures of immunostained liver sections against IL-6 (Low magnification ×100 bar 100, high magnification ×400 bar 50) showing: control group showed negative staining (**A-a**); NASH group showed marked positive brown expression against IL-6 in hepatocytes (*black arrows*) (**B-b**); PTX group showed decreased positive brown expression in hepatocytes (*black arrows*) in treated groups with a single drug (**C-c**); PTX+KP group showed much more decreased of positive brown expression in hepatocytes (*black arrows*) in treated groups with drug combinations (**D-d**). IHC counterstained with Mayer's hematoxylin. **E**, Statistical analysis of positive IHC expression scores of IL-6 with the Kruskal-Wallis' method (found to be non-parametric data) followed by Dunn's test showed a significant increase in NASH compared to the control group. Significant reductions of positive IHC expression scores of IL-6 in treated groups with drug combinations to be the lowest in treated group with PTX+KP. Small alphabetical letters mean significant when $p<0.05$. Data are presented as mean ± SD, $p<0.001$, n=8. a: significant *vs.* control group, b: significant *vs.* NASH group, c: significant *vs.* PTX group.

and TC levels than the untreated NASH group, these findings are consistent with the previous research[38]. The combined treatment of PTX d with KP might reduce NASH-induced dyslipidemia. This effect was consistent with prior results that PTX may lower body weight by modifying liver metabolites and lipid indices *via* modulation of the critical metabolic pathways[39].

AMPK regulates cellular energy balance by controlling proliferation, metabolic reprogramming, autophagy, apoptosis, and cell differentiation. The kinase is triggered in response to ATP-depleting stresses such as low glucose, hypoxia, ischemia, and heat shock. It also controls cellular energy balance and metabolism of fatty acids through the fatty acid synthesis pathway[40].

SREBPs are transcription factors that control the expression of genes involved in the biosynthesis of cholesterol, fatty acid synthesis, triglyceride synthesis, and phospholipid synthesis. *FAS* and *ACC*, two genes involved in triglyceride synthesis and accumulation, are regulated by SREBP-1c. Consequently, activation of AMPK reduces ACC and FAS production by downregulating SREBP-1c[41].

To put even more focus on AMPK, treatment with PTX alone or in combination with KP, stimulated AMPK while decreasing SERBP-1c gene expression in the current study. These results were confirmed with previous research[42] found that combining two medications greatly increased AMPK gene expression compared to each treatment alone.

Indeed, reduced AMPK activity in NASH may stimulate NF-κB signaling[43]. PTX has previously been found[44] to decrease the expression of the NF-κB gene in several types of cells. It is worth noting that PTX and KP may lower insulin resistance by inhibiting NF-κB and increasing AMPK expression, which explains why glucose and insulin levels have decreased. Moreover, PTX therapy reduced insulin resistance and stabilized plasma

glucose and insulin levels. However, the combination therapy of KP+PTX resulted in an even higher reduction.

In metabolic liver disease, apoptosis and necroptosis are critical regulatory processes. As a result, human NASH is one of the only human illnesses in which necroptosis is initiated *in vivo* without inhibiting apoptosis. Animals missing RIPK3 were also protected in an alcoholic liver disease model, adding to the growing evidence that necroptosis is a critical metabolic process of cell death in the liver[45].

In the case of NASH in the current study, both PTX alone and in combination-treated animals showed a substantial reduction in RIPK3 expression targeting necroptosis, implying that this could be a promising and targeted treatment strategy. Similar to the previous work[4], blocking RIPK3 in NASH mice given a choline-deficient diet (CD-D) enhanced adipocyte death and systemic insulin resistance.

Proinflammatory cytokines, such as IL-1, IL-6, and TNF-α are produced in greater quantities, which characterize fatty liver disease; earlier research[46] has shown that TNF-α plays a vital role in the evolution of NASH in people. TNF-α and IL-6 have been linked to the development of NAFLD. In the current study, the considerable decrease and restoration of proinflammatory cytokines in the PTX and PTX+KP co-therapy groups corroborated our findings[47].

ROS also causes the production of cytokines that cause hepatocyte apoptosis, such as TNF-α, TGF-β, and IL-8, suggesting that TNF-α and IL-6 may play a role in the development of NASH. The considerable decrease and restoration of proinflammatory cytokines in the PTX and PTX+KP co-therapy groups supported our findings[6].

Some researchers[48] used hepatocyte-specific caspase-8 deletion mice to demonstrate that deleting this caspase reduced hepatocyte mortality, proinflammatory cytokine production, and hepatic infiltration in MCD-fed animals.

Caspase-8 is not only required for apoptosis to occur but also acts as a crucial switch that guides cell death to certain forms of cell death: caspase-8 activation promotes apoptosis, whereas inhibition of caspase-8 tips the balance toward necroptosis[49]. An increasing amount of data[50] shows that enhanced phagocyte apoptosis is crucial in NASH-related liver inflammation and fibrogenesis.

Caspases can be activated by either the death receptor-dependent or mitochondrial-dependent pathways. Cells die only when anti-apoptotic signals, particularly NF-κB activity, are reduced. Interestingly, our investigation found that PTX alone and combined with KP significantly reduced caspase 8 expression[51].

Furthermore, MLKL phosphorylation was assumed to be one of the irreversible biochemical pathways that result in necroptosis[52]. P-MLKL expression was significantly reduced in PTX and PTX+KP-treated mice and co-treatment. This enhanced cellular export of p-MLKL suggests that activated MLKL is self-limiting; hence, necroptosis is limited[53].

Energy homeostasis in hepatocytes is controlled by mitochondrial FAO, electron transport, ATP production, and ROS[54]. Mitochondrial dysfunction contributes to an imbalance of prooxidant and antioxidant processes, resulting in lipid accumulation and excessive ROS generation. The latter induces the activation of inflammatory mediators and signaling pathways in NASH patients, increasing inflammation, ROS generation, and oxidative DNA damage[43]. ROS and lipid peroxidation can deplete antioxidant enzymes, exposing the liver to oxidative stress[55].

MDA is a lipid peroxidation breakdown product, and its existence represents the amount of oxygen free radicals in tissues[56]. SOD is a major macromolecular antioxidant whose activity signifies a tissue's ability to scavenge oxygen free radicals. It has been demonstrated that MDA increases while SOD decreases gradually with age. In NAFLD patients, mitochondrial dysfunction is crucial for progressing from basic steatosis to NASH[57].

Gpx is an enzyme family that forms mammals' major antioxidant defense mechanism. The most prevalent GPx isoenzyme, 7 GPx1, is also expressed in the liver[58]. Our results showed that PTX and markedly in PTX+KP significantly decrease mice serum MDA levels and increase serum SOD and GPx.

Conclusions

The current study proved that pentoxifylline, alone or in association with Kaempferol, is effective and promising in treating and preventing NASH by different mechanisms through downregulating caspase 8, pMLKL and RIPK3 which stimulate apoptosis and necroptosis pathways. Moreover, the reduction of cytokines like TNF-α, IL-6, NF-κB and oxidative stress, as well as acting through the decrease of lipogenesis genes such as AMPK and SREBP-1 all alleviates NASH.

Conflict of Interest
The Authors declare that they have no conflict of interests.

Funding
The authors declare no financial support.

Ethics Approval
Our manuscript data were collected from animals, and the ethical criteria for the care and use of laboratory animals (National Research Council) were followed in the housing and administration of the animals, as approved by the Research Ethical Committee, Faculty of Pharmacy, Suez Canal University, Egypt (Approval number: 202007PHDA1).

Availability of Data and Materials
All materials and data, as well as the statements they support, are available upon reasonable request from authors and are matched to field requirements for transparency.

Authors' Contribution
All authors contributed significantly to the work reported, whether in the conception, study design, execution, data acquisition, analysis, and interpretation, or in all these areas; participated in the drafting, revising, or critical review of the article; gave final approval of the version to be published; agreed on the journal to which the article was submitted; and agreed to be accountable for all aspects of the work.

References

1) Drucker D. Diabetes, obesity, metabolism, and SARS-CoV-2 infection: the end of the beginning. Cell Metab 2021; 33: 479-498.
2) Burra P, Becchetti C, Germani G. NAFLD and liver transplantation: Disease burden, current management, and future challenges. JHEP Rep 2020; 2: 1-12.
3) Parthasarathy G, Revelo X, Malhi H. Pathogenesis of Nonalcoholic Steatohepatitis: An Overview. Hepatol Commun 2020; 4: 478-492.
4) Shojaie L, Iorga A, Dara L. Cell Death in Liver Diseases: A Review. Int J Mol Sci 2020; 21: 9682-9690.
5) Chen L, Cao Z, Yan L, Ding Y, Shen X, Liu K, Xiang X, Xie Q, Zhu C, Bao S, Wang H. Circulating Receptor-Interacting Protein Kinase 3 Are Increased in HBV Patients With Acute-on-Chronic Liver Failure and Are Associated With Clinical Outcome. Front Physiol 2020; 11: 1-6.
6) Hao F, Cubero FJ, Ramadori P, Liao L, Haas U, Lambertz D, Sonntag R, Bangen JM, Gassler N, Hoss M, Streetz KL, Reissing J, Zimmermann HW, Trautwein C, Liedtke C, Nevzorova YA. Inhibition of Caspase-8 does not protect from alcohol-induced liver apoptosis but alleviates alcoholic hepatic steatosis in mice. Cell Death Dis 2017; 8: e3152.
7) Godoy F, Silva Júnior S, Valerio C. NAFLD as a continuum: from obesity to metabolic syndrome and diabetes. Diabetology & metabolic syndrome 2020; 12: 60-70.
8) Sousa-Lima I, Kim H, Jones J, Kim YB. Rho-Kinase as a Therapeutic Target for Nonalcoholic Fatty Liver Diseases. Diabetes Metab J 2021; 45: 655-674.
9) Li Y, Xu S, Mihaylova MM, Zheng B, Hou X, Jiang B, Park O, Luo Z, Lefai E, Shyy J Y, Gao B, Wierzbicki M, Verbeuren TJ, Shaw RJ, Cohen RA, Zang M. AMPK phosphorylates and inhibits SREBP activity to attenuate hepatic steatosis and atherosclerosis in diet-induced insulin-resistant mice. Cell Metab 2011; 13: 376-388.
10) Karkucinska-Wieckowska A, Simoes M, Kalinowski P, Lebiedzinska M, Zieniewicz K, Milkiewicz P, Gorska M, Pinton P, Malik AN, Krawczyk M, Oliveira PJ, Wieckowski M. Mitochondria, oxidative stress and nonalcoholic fatty liver disease: A complex relationship. Eur J Clin Invest 2022; 52: 1-15.
11) Irazabal M, Torres E. Reactive Oxygen Species and Redox Signaling in Chronic Kidney Disease. Cells 2020; 9: 1-20.
12) Du J, Ma Y, Yu C, Li Y. Effects of pentoxifylline on nonalcoholic fatty liver disease: a meta-analysis. World J Gastroenterol 2014; 20: 569-577.
13) Caporali S, De Stefano A, Calabrese C, Giovannelli A, Pieri M, Savini I, Tesauro M, Bernardini S, Minieri M, Terrinoni A. Anti-Inflammatory and Active Biological Properties of the Plant-Derived Bioactive Compounds Luteolin and Luteolin 7-Glucoside. Nutrients 2022; 14: e1155.
14) Kluska M, Juszczak M, Żuchowski J, Stochmal A, Woźniak K. Effect of Kaempferol and Its Glycoside Derivatives on Antioxidant Status of HL-60 Cells Treated with Etoposide. Molecules 2022; 27: 1-14.
15) Ye J, Chao J, Chang M, Peng H, Cheng Y, Liao W, Pao L. Pentoxifylline ameliorates non-alcoholic fatty liver disease in hyperglycaemic and dyslipidaemic mice by upregulating fatty acid beta-oxidation. Sci Rep 2016; 6: 1-13.
16) Owada Y, Tamura T, Tanoi T, Ozawa Y, Shimizu Y, Hisakura K, Matsuzaka T, Shimano H, Nakano N, Sakashita S, Matsukawa T, Isoda H, Ohkohchi N. Novel non-alcoholic steatohepatitis model with histopathological and insulin-resistant features. Pathol Int 2018; 68: 12-22.
17) Hsiao J, Chiou C, Jiang J, Lee M, Hsieh J, Kuo K. Pioglitazone Enhances Cytosolic Lipolysis, beta-oxidation and Autophagy to Ameliorate Hepatic Steatosis. Sci Rep 2017; 7: 1-11.
18) Trinder P. Determination of blood glucose using an oxidase-peroxidase system with a non-carcinogenic chromogen. J Clin Pathol 1969; 22: 158-161.

19) Matthews D, Hosker J, Rudenski A, Naylor B, Treacher D, Turner R. Homeostasis model assessment: insulin resistance and β-cell function from fasting plasma glucose and insulin concentrations in man. Diabetologia 1985; 28: 412-419.

20) Rao X, Huang X, Zhou Z, Lin X. An improvement of the 2ˆ(-delta delta CT) method for quantitative real-time polymerase chain reaction data analysis. Biostat Bioinforma Biomath 2013; 3: 71-85.

21) Zaidi S, Hoda M, Tabrez S, Ansari S, Jafri A, Shahnawaz Khan M, Hasan S, Alqahtani M H, Mohammed Abuzenadah A, Banu N. Protective Effect of Solanum nigrum Leaves Extract on Immobilization Stress Induced Changes in Rat's Brain. Evid Based Complement Alternat Med 2014; 2014: 1-6.

22) Ray L, Panda A, Mishra S, Pattanaik A, Adhya T, Suar M, Raina V. Purification and characterization of an extracellular thermo-alkali stable, metal tolerant chitinase from Streptomyces chilikensis RC1830 isolated from a brackish water lake sediment. Biotechnol Rep 2019; 21: e00311.

23) Buege JA, Aust SD. Microsomal lipid peroxidation. Methods Enzymol 1978; 52: 302-310.

24) Singh N, Jain N, Kumar R, Jain A, Singh NK, Rai V. A comparative method for protein extraction and 2-D gel electrophoresis from different tissues of Cajanus cajan. Front Plant Sci 2015; 6: 1-7.

25) Kleiner DE, Brunt EM, Van Natta M, Behling C, Contos MJ, Cummings OW, Ferrell LD, Liu YC, Torbenson MS, Unalp-Arida A, Yeh M, McCullough AJ, Sanyal AJ. Design and validation of a histological scoring system for nonalcoholic fatty liver disease. Hepatology 2005; 41: 1313-1321.

26) Butler T, Paul J, Chan E , Smith R, Tolosa J. Misleading Westerns: Common Quantification Mistakes in Western Blot Densitometry and Proposed Corrective Measures. Biomed Res Int 2019; 2019: 1-15.

27) Pan, X, Ma X, Jiang Y, Wen J, Yang L, Chen, D, Cao, X., Peng C. A Comprehensive Review of Natural Products against Liver Fibrosis: Flavonoids, Quinones, Lignans, Phenols, and Acids. Evidence-based complementary and alternative medicine 2020; 5; 1-19.

28) Sotiropoulou M, Katsaros I, Vailas M, Lidoriki I, Papatheodoridis GV, Kostomitsopoulos NG, Valsami G, Tsaroucha A, Schizas D. Nonalcoholic fatty liver disease: The role of quercetin and its therapeutic implications. Saudi J Gastroenterol 2021; 27: 319-330.

29) Sandoval V, Sanz H, Arias G, Marrero P, Haro D, Relat J. Metabolic Impact of Flavonoids Consumption in Obesity: From Central to Peripheral. Nutrients 2020; 12: 1-54.

30) Wang M, Sun J, Jiang Z, Xie W, Zhang X. Hepatoprotective effect of kaempferol against alcoholic liver injury in mice. Am J Chin Med 2015; 43: 241-254.

31) Luo M, Dong L, Li J, Wang Y, Shang B. Protective effects of pentoxifylline on acute liver injury induced by thioacetamide in rats. Int J Clin Exp Pathol 2015; 8: 8990-8996.

32) Jeschke M. The hepatic response to thermal injury: is the liver important for postburn outcomes? Mol Med 2009; 15: 337-351.

33) Paul J. Recent advances in non-invasive diagnosis and medical management of non-alcoholic fatty liver disease in adult. Egyptian Liver Journal 2020; 10: 1-18.

34) Ćulafić M, Vezmar-Kovačević S, Dopsaj V, Olui B, Bidžić N, Miljković B, Ćulafić Đ. Pentoxifylline with metformin treatment improves biochemical parameters in patients with nonalcoholic steatohepatitis. J Med Biochem 2020; 39: 290-298.

35) Luo C, Yang H, Tang C, Yao G, Kong L, He H, Zhou Y. Kaempferol alleviates insulin resistance via hepatic IKK/NF-κB signal in type 2 diabetic rats. Int Immunopharmacol 2015; 28: 744-750.

36) Zou F, Wang L, Liu H, Wang W, Hu L, Xiong X, Wu L, Shen Y, Yang R. Sophocarpine Suppresses NF-κB-Mediated Inflammation Both In Vitro and In Vivo and Inhibits Diabetic Cardiomyopathy. Front Pharmacol 2019; 10: 1219-1219.

37) Perakakis N, Chrysafi P, Feigh M, Veidal SS, Mantzoros CS. Empagliflozin Improves Metabolic and Hepatic Outcomes in a Non-Diabetic Obese Biopsy-Proven Mouse Model of Advanced NASH. Int J Mol Sci 2021; 22: 1-12.

38) Mansour R, Mansour F, Naghipour M, Joukar F. Biochemical markers and lipid profile in nonalcoholic fatty liver disease patients in the PERSIAN Guilan cohort study (PGCS), Iran. J Family Med Prim Care 2019; 8: 923-928.

39) Yang H, Suh D, Kim D , Jung E, Liu K, Lee C, Park C. Metabolomic and lipidomic analysis of the effect of pioglitazone on hepatic steatosis in a rat model of obese Type 2 diabetes. Br J Pharmacol 2018; 175: 3610-3625.

40) Chuang HC, Chou CC, Kulp SK, Chen CS. AMPK as a potential anticancer target - friend or foe? Curr Pharm Des 2014; 20: 2607-2618.

41) Wang Q, Sun J, Liu M, Zhou Y, Zhang L, Li Y. The New Role of AMP-Activated Protein Kinase in Regulating Fat Metabolism and Energy Expenditure in Adipose Tissue. Biomolecules 2021; 11: 1-15.

42) Zhao P, Saltiel A. From overnutrition to liver injury: AMP-activated protein kinase in nonalcoholic fatty liver diseases. J Biol Chem 2020; 295: 12279-12289.

43) Chen Z, Tian R, She Z, Cai J, Li H. Role of oxidative stress in the pathogenesis of nonalcoholic fatty liver disease. Free Radic Biol Med 2020; 152: 116-141.

44) Albensi B. What Is Nuclear Factor Kappa B (NF-kappa) Doing in and to the Mitochondrion? Front Cell Dev Biol 2019; 7: 154-162.

45) Schwabe F, Luedde T. Apoptosis and necroptosis in the liver: a matter of life and death. Nat Rev Gastroenterol Hepatol 2018; 15: 738-752.

46) Niederreiter L, Tilg H. Cytokines and fatty liver diseases. Liver Research 2018; 2: 14-20.

47) Friedman S L, Neuschwander-Tetri BA, Rinella M, Sanyal AJ. Mechanisms of NAFLD development and therapeutic strategies. Nat Med 2018; 24: 908-922.

48) Hatting M, Zhao G, Schumacher F, Sellge G, Al Masaoudi M, Gaβler N, Boekschoten M, Müller M, Liedtke C, Cubero F J, Trautwein C. Hepatocyte caspase-8 is an essential modulator of steatohepatitis in rodents. Hepatology 2013; 57: 2189-2201.

49) Fritsch M, Günther S, Schwarzer R, Albert M, Schorn F, Werthenbach J P, Schiffmann L M, Stair N, Stocks H, Seeger J M, Lamkanfi M, Krönke M, Pasparakis M, Kashkar H. Caspase-8 is the molecular switch for apoptosis, necroptosis and pyroptosis. Nature 2019; 575: 683-687.

50) Huby T, Gautier E. Immune cell-mediated features of non-alcoholic steatohepatitis. Nature Reviews Immunology 2022; 22: 429-443.

51) Del Re D, Amgalan D, Linkermann A, Liu Q, Kitsis R. Fundamental Mechanisms of Regulated Cell Death and Implications for Heart Disease. Physiol Rev 2019; 99: 1765-1817.

52) Gong Y-N, Guy C, Crawford J, Green D. Biological events and molecular signaling following MLKL activation during necroptosis. Cell cycle 2017; 16: 1748-1760.

53) Samson L, Zhang Y, Geoghegan D, Gavin XJ, Davies A, Mlodzianoski J, Whitehead W, Frank D, Garnish E, Fitzgibbon C, Hempel A, Young N, Jacobsen V, Cawthorne W, Petrie J, Faux C, Shield-Artin K, Lalaoui N, Hildebrand M, Silke J, Rogers L, Lesesne G, Hawkins D, Murphy JM. MLKL trafficking and accumulation at the plasma membrane control the kinetics and threshold for necroptosis. Nat Commun 2020; 11: 1-17.

54) Legaki A I, Moustakas, II, Sikorska M, Papadopoulos G, Velliou RI, Chatzigeorgiou A. Hepatocyte Mitochondrial Dynamics and Bioenergetics in Obesity-Related Non-Alcoholic Fatty Liver Disease. Curr Obes Rep 2022; 11: 126-143.

55) Sadasivam N, Kim YJ, Radhakrishnan K, Kim DK. Oxidative Stress, Genomic Integrity, and Liver Diseases. Molecules 2022; 27: 1-18.

56) Ayala A, Muñoz M, Argüelles S. Lipid peroxidation: production, metabolism, and signaling mechanisms of malondialdehyde and 4-hydroxy-2-nonenal. Oxid Med Cell Longev 2014; 2014: 1-31.

57) Arya A, Azarmehr N, Mansourian M, Doustimotlagh A. Inactivation of the superoxide dismutase by malondialdehyde in the nonalcoholic fatty liver disease: a combined molecular docking approach to clinical studies. Arch Physiol Biochem 2021; 127: 557-564.

58) Shen Y, Huang H, Wang Y, Yang R, Ke X. Antioxidant effects of Se-glutathione peroxidase in alcoholic liver disease. J Trace Elem Med Biol 2022; 74: 127048-127060.